Biochemical and Biophysical Research Communications 391 (2010) 123–128

Contents lists available at ScienceDirect

Biochemical and Biophysical Research Communications

journal homepage: www.elsevier.com/locate/ybbrc

Mitochondrial intermediate peptidase: Expression in *Escherichia coli* and improvement of its enzymatic activity detection with FRET substrates

Marcelo F. Marcondes [a], Ricardo J.S. Torquato [b], Diego M. Assis [a], Maria A. Juliano [a], Mirian A.F. Hayashi [c], Vitor Oliveira [a,*]

[a] Department of Biophysics, Federal University of São Paulo, São Paulo 04044-020, SP, Brazil
[b] Department of Biochemistry, Federal University of São Paulo, São Paulo 04044-020, SP, Brazil
[c] Department of Pharmacology, Federal University of São Paulo, São Paulo 04044-020, SP, Brazil

ARTICLE INFO

Article history:
Received 29 October 2009
Available online 10 November 2009

Keywords:
Peptidase
Mitochondria
Bacterial expression
Enzymatic activity
FRET substrate

ABSTRACT

In the present study, soluble, functionally-active, recombinant human mitochondrial intermediate peptidase (*h*MIP), a mitochondrial metalloendoprotease, was expressed in a prokaryotic system. The *h*MIP fusion protein, with a poly-His-tag (6× His), was obtained by cloning the coding region of *h*MIP cDNA into the pET-28a expression vector, which was then used to transform *Escherichia coli* BL21 (DE3) pLysS. After isolation and purification of the fusion protein by affinity chromatography using Ni–Sepharose resin, the protein was purified further using ion exchange chromatography with a Hi-trap resource Q column. The recombinant *h*MIP was characterized by Western blotting using three distinct antibodies, circular dichroism, and enzymatic assays that used the first FRET substrates developed for MIP and a series of protease inhibitors. The successful expression of enzymatically-active *h*MIP in addition to the FRET substrates will contribute greatly to the determination of substrate specificity of this protease and to the development of specific inhibitors that are essential for a better understanding of the role of this protease in mitochondrial functioning.

Introduction

Despite mitochondria having its own genome, most of the mitochondrial proteins are synthesized outside this organelle under the direction of the nuclear DNA [1]. Several proteins that are targeted to the mitochondrial matrix, inter-membrane space or internal membrane are synthesized as precursor proteins that have an extended N-terminus that is removed by specific peptidases present in this organelle [2]. The mitochondrial processing peptidase (MPP; EC 3.4.24.64) is the major enzyme responsible for the processing of the proteins that have been addressed to the inner membrane, inter-membrane space or mitochondrial matrix. Most of proteins addressed to the mitochondrial matrix and inner membrane require only the action of the MPP. In the mitochondrial matrix some proteins also require a second, sequential cleavage after the action of the MPP, and this has been attributed to the mitochondrial intermediate peptidase (MIP; EC 3.4.24.59) that removes eight residues from the newly-generated N-terminus [3–6].

MIP was identified in rats (*r*MIP) [5,7], humans (*h*MIP) [8], *Saccharomyces cerevisiae* (*y*MIP) [9] and *Schizophillum commune* (*s*MIP) [10]. In all cases, it was found as a soluble monomer of about 75 kDa with the canonical zinc ion ligand motif, HEXXH. Site-point mutation studies confirmed the functionality of this metalloprotease motif [11]. MIP is encoded by a nuclear gene, and thus needs to be transported to the mitochondria. It also presents a signal sequence (of 33, 35 and 37 residues for *r*MIP, *h*MIP and *y*MIP, respectively) that is cleaved by MPP. MIP is expressed predominately in tissues that consume oxygen at a high rate, i.e., in heart and skeletal muscle, and in several regions of the brain [12].

In the present work, we describe the expression of *h*MIP in fusion with a hexahistidine tag in *Escherichia coli*. The expression and purification conditions were optimized, and the final yield of homogeneous active *h*MIP was ~1 mg/L. The advantages and disadvantages of this new method for MIP expression are discussed herein. The protein was structurally characterized by its immunoreactivity with three different antibodies, by fluorescence and circular dichroism analysis. The effects of different protease inhibitors and DTT on *h*MIP enzymatic activity were also investigated. For these activity assays a new strategy to measure the MIP activity using FRET substrates was developed and it is also described.

Abbreviations: PMSF, phenylmethanesulfonylfluoride; E-64, (2*S*,3*S*)-3-(*N*-{(*S*)-1-[*N*-(4-guanidinobutyl)carbamoyl]3-methylbutyl}carbamoyl)oxirane-2-carboxylic acid; JA-2, *N*-[1-(*R*,*S*)-carboxy-3-phenylpropyl]Ala-Aib-Tyr-*p*-aminobenzoate; FRET, fluorescence resonance energy transfer.

* Corresponding author. Address: Department of Biophysics, Universidade Federal de São Paulo (UNIFESP), Rua 3 de maio, 100 – INFAR 2nd floor, São Paulo, Brazil. Fax: +55 11 55764450.
E-mail address: vitor@biofis.epm.br (V. Oliveira).

0006-291X/$ - see front matter © 2009 Elsevier Inc. All rights reserved.
doi:10.1016/j.bbrc.2009.11.014

Material and methods

Construction of the expression vector

The *h*MIP cDNA fragment (~2000 bp) was amplified by PCR from the clone, ID 4053687 from the Mammalian Gene Collection (MGC) (Invitrogen). The primers 5′GCTAGCGTGGGCGCCGCCTT CAAT3′ and 5′TGCGGCCGCTTATTCAGAATCCATGAG3′ were used for in-frame cloning with a poly-histidine tag at the N-terminus, and the primers 5′GCTAGCGTGGGCGCCGCCTTCAAT3′ and 5′CCC GGGTTATTCAGAATCCATGAGGAAAGTTTCGAAGTCCAG3′ were used to prepare the construct with a poly-His-tag at both the N- and C-termini. The PCR amplification was carried denaturing the template at 95 °C for 2 min, followed by 35 cycles of amplification (95 °C for 30 s, 60 °C for 1 min and 72 °C for 2.5 min), with a final reaction at 72 °C for 5 min. The PCR product obtained was subcloned into the T/A vector pTZ57-R/T (InsTAclone™ PCR Cloning Kit – Fermentas), and the recombinant colonies were selected by PCR amplification using the specific primers described above. Plasmid DNA from the positive clones was purified and double-digested with NheI and NotI restriction enzymes to construct the version with the poly-histidine tag at the N-terminus. The DNA was double-digested with NheI and SmaI to construct the version with the poly-histidine tag at the N- and C-termini. The expression vector pET-28 (Novagen, USA) was also digested using the same enzymes. Then, the purified (Wizard SV Gel and PCR Clean UP System (Promega)) double-digested expression vectors (140 fmol) and the cDNA inserts coding for *h*MIP (40 fmol) were incubated with 3 units of T4 DNA ligase (Promega) for 12 h at 20 °C. This ligation mixture containing the pET-28–MIP construct was used to transform chemically-competent *E. coli* DH5-alpha, which were then plated on solid LB medium containing 50 μg/mL kanamycin. The correct placing of the cDNA insert coding for *h*MIP in the reading frame of the expression vector was confirmed by sequencing amplification products from the colony PCR reactions using an ABI Prism 310 Genetic Analyzer and Dynamic Sequencing reagents (Applied Biosystems).

Expression of recombinant hMIP

E. coli BL21 (DE3) pLysS (Novagen) was used as the host for the expression of the *h*MIP gene. Chemically-competent *E. coli* BL21(DE3) cells were transformed with the expression construct. The transformed *E. coli* cells were incubated overnight at 30 °C in 10 mL of Luria-broth (LB) medium containing kanamycin (50 μg/mL) and chloramphenicol (50 μg/mL) under agitation at 150 rpm. These cells were then transferred to 1 L of fresh LB medium at 30 °C and 150 rpm, until the culture density reached an OD_{550} of 0.4. The temperature was then reduced to 20 °C until the culture density reached an OD_{550} of 0.6–0.7. At this point, isopropyl β-D-1-thiogalactopyranoside (IPTG) was added to a final concentration of 0.1 mM, and the culture was incubated at 20 °C for 14–16 h. Then, the bacterial cells were harvested by centrifugation at 5000 rpm, for 10 min, at 4 °C. The pellet was stored at −70 °C.

Purification of the recombinant hMIP

Cell lysis. The pellet was resuspended in 20 mL of binding buffer (50 mM NaH_2PO_4, 500 mM NaCl, 20 mM imidazole, pH 8.0), and lysozyme was added to a final concentration of 1 mg/mL. The suspension was then incubated on ice for 30 min. RNase and DNase (to a final concentration of 5 μg/mL each), and 2 mL of 0.2% Triton X-100, were then added. After incubation, the solution was then centrifuged at 15,000 rpm for 20 min, and the supernatant was recovered.

The first purification step – Ni–Sepharose high performance desalting prep. The supernatant was loaded into a Ni–Sepharose high performance chromatography column (GE Healthcare) that had been equilibrated with binding buffer at a flow rate of 0.5 mL/min. The column was washed with 5 mL of binding buffer, and the recombinant *h*MIP was eluted using a segmented step elution with different concentrations of imidazole (50, 100 and 150 mM) in binding buffer (20 mM NaH_2PO_4 pH 8.0, 500 mM NaCl). The column was then washed with 500 mM of imidazole, and each step was performed using 5 mL of elution buffer. The recombinant protein eluted between 100 and 150 mM imidazole. These fractions, ~8–10 mL each, were collected and loaded onto a desalting prep column (GE Healthcare) for desalinization, and the fractions containing *h*MIP were recovered.

The second purification step – resource Q Sepharose. The fractions containing *h*MIP were loaded into a resource Q column (1 mL) that had been equilibrated with TB buffer (50 mM Tris, pH 7.4) at flow rate of 1.0 mL/min. The column was then washed with 6 mL of TB buffer. The recombinant *h*MIP was eluted using 40 mL of a linear gradient with TBS buffer (50 mM Tris–HCl, pH 7.4, 500 mM NaCl). Recombinant *h*MIP eluted between 80 and 200 mM NaCl. These fractions were collected and aliquots were analyzed using SDS/PAGE. The fractions containing pure, recombinant *h*MIP were concentrated using an Amicon filtration unit (Millipore Corp.), equipped with a 50 kDa exclusion membrane, and the recovered protein was stored in TBS buffer at −70 °C.

Circular dichroism (CD)

Far-UV CD spectra were recorded on a Jasco J-810 spectropolarimeter. The spectrometer conditions typically included a sensitivity of 100 mdeg, a resolution of 0.5 nm, a response time of 4 s, a scan rate of 20 nm/min, and 4 accumulations at 37 °C.

Western blotting

The protein samples that had been separated by SDS/PAGE electrophoresis (10%) were eletro-transferred to a nitrocellulose membrane. The nitrocellulose membrane was incubated with the primary antibody solutions for ~12 h at 20 °C. The primary antibodies used here were raised against full-length *h*MIP (Protein-Tech.), against the *h*MIP N-terminal synthetic peptide (Abgent), and against the poly-histidine tag (Invitrogen). Then, the membrane was incubated with the peroxidase-conjugated anti-rabbit IgG secondary antibody (diluted 1:1000) for 1 h at 20 °C. Finally, the membrane was developed using a peroxidase substrate, 4-chloro-1 naphthol (Sigma).

Peptide synthesis

Highly sensitive FRET peptides were synthesized by solid-phase procedures, as described elsewhere [13].

Enzymatic activity assay

Recombinant *h*MIP was assayed by incubating the synthetic peptide with the sequence of bradykinin (50 μM (Sigma)) with 11 nM of *h*MIP in TBS buffer (50 mM Tris, pH 7.4, 100 mM NaCl) at 37 °C. The final volume was 2 mL. Each hour, 250-μL aliquots were collected, for 8 h, and the reactions were stopped by adding 4 μL 1 M HCl. The reactions were monitored using analytical high performance liquid chromatography (HPLC).

Hydrolysis of the FRET peptides Abz-RPPGFSPFRQ-EDDnp and Abz-GFSPFRQ-EDDnp also used as substrates for *h*MIP was monitored spectrofluorometrically in a Shimadzu RF-5301PC spectrofluorometer with excitation and emission wavelengths of 320 and

420 nm, respectively. The rate of increase in fluorescence was converted into moles of substrate hydrolyzed per second based on the fluorescence curves of standard peptide solutions before and after total enzymatic hydrolysis. The enzyme concentration for initial rate determinations was chosen so that <10% of the substrate was hydrolyzed. The activity was measured in the absence or in the presence of the assayed inhibitors and DTT.

Determination of peptide cleavage sites

The peptide bonds that were cleaved were identified by using mass spectrometry (LCMS-2010 EV Shimadzu, Tokyo, Japan) and/or peptide sequencing using a PPSQ-23 protein sequencer (Shimadzu, Tokyo, Japan).

Mass spectrometric analysis of hMIP

The molecular mass of the recombinant *h*MIP was determined using the positive ionization mode in MALDI-TOF mass spectrometry (Microflex LT, Bruker), using alpha-cyano-4-hydroxycinnamic acid as the matrix.

Results and discussion

Construction of the expression vector

The recombinant MIP that was obtained had a hexahistidine tag at its N-terminus in the place of the residues that correspond to the mitochondrial signal sequence. However, the histidine tag at the N-terminus did not alter the enzymatic activity of the recombinant MIP, as removal of the tag by thrombin did not affect the enzymatic activity (data not shown). Therefore, we used the fusion form of the *h*MIP with the His-tag in this work. We also tried another construct, taking advantage of the different reading frame of the vector (pET-28b). This allowed the expression of an active form of *h*MIP that had the histidine tag at both extremities, i.e., the N- and C-termini, and this *h*MIP fusion showed the same kinetic profile for the peptide substrates that we tested (data not shown). Considering that MIP has the same overall folding of its homologous the thimet oligopeptidase (EC 3.4.24.15; TOP) and neurolysin (EC 3.4.24.16; NEL) these observations are supported by the positions of the N- and C-termini in the 3D structures of these peptidases [14,15]. However, unlike TOP and NEL, MIP can act on large proteins [4–6]. This is very intriguing, as it is believed that the folding of TOP and NEL prevents the hydrolysis of large substrates by these peptidases. This is because their active sites reside at the end of a "deep channel" [14,15]. It is not known to what extent the structure of MIP is different from TOP and NEL, since the 3D structure of MIP has not been determined to date.

Expression and purification of recombinant hMIP

The average yield of purified protein obtained using the *h*MIP expression protocol described in the Materials and Methods section, was approximately 1 mg per liter of culture medium. The tight controlled temperature during the expression induction step as the IPTG concentration that must be lower than 0.1 mM are critical for a successful protein expression and thus to the final yield. Fig. 1 shows the results of the SDS/PAGE analysis (Fig. 1A) of the two purification steps used and the respective chromatograms (Fig. 2B and C). As assessed by SDS/PAGE, the purification protocol yielded an apparently homogenous protein sample (purity >95%). We also tested gel filtration using Sephadex 75 or 200 resin (data not shown) after the affinity chromatography step, instead of an ionic exchange step. However, the best results were obtained using the resource Q column (Fig. 1C).

There is a previous description of a methodology for MIP production that consists in the purification of the protein from mitochondria of transformed *S. cerevisiae*, which resulted in the expression of MIP fused with a *myc*-tag sequence at its C-terminus [10,11]. The protein was purified from the mitochondrial isolated fractions because the extended N-terminus signal sequence directs the MIP-*myc* to mitochondria where this protein is then processed by MPP. The *myc*-tag facilitates the purification in a column with immobilized anti-*myc*. Therefore, this methodology can also be successfully applied for *h*MIP production. However, the alternative strategy described in the present work is easier and has the convenient advantages of a bacterial expression over a yeast expression in a laboratory scale. For an enzyme like *h*MIP some additional advantages can be pointed, for instance, when mutants or some other modifications such as the addition of different tags is aimed. As well known, for each desired modification new transformation/selection processes are required, and these critical steps are highly time-consuming processes in yeast systems, on the other hand they are simple and effortless in bacteria.

The primary structure and immunochemical characterization of hMIP

To confirm the molecular mass of the obtained recombinant *h*MIP, the molecular weight was determined using SDS–PAGE and MALDI-TOF mass spectrometry. The mass spectrometry indicated a main peak of 78,644 Da, in agreement with the theoretical size for the deduced amino acid sequence (78,750 Da), considering the error of the technique using the external calibration. Moreover,

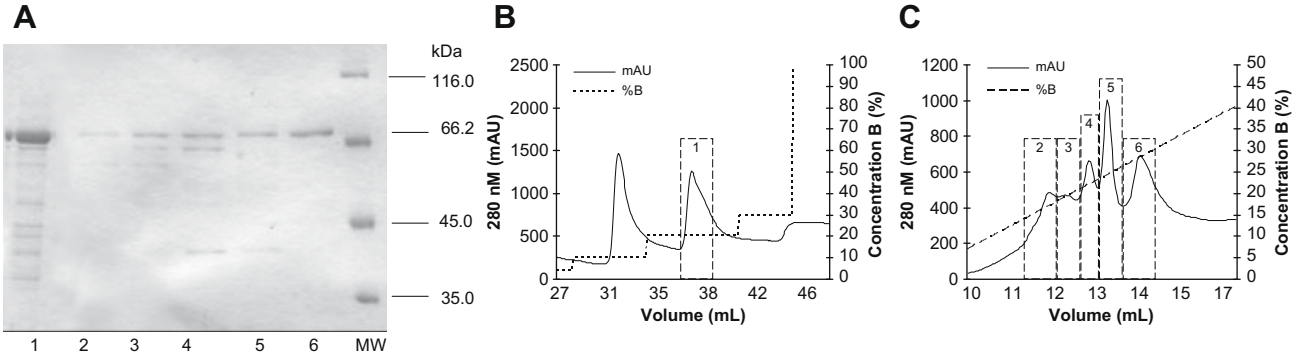

Fig. 1. Recombinant *h*MIP purification. (A) SDS/PAGE analysis of the aliquots taken from the purification steps employed for *h*MIP purification. Lane 1 – aliquot from the affinity chromatography using Ni–Sepharose high performance as showed in (B). Lanes 2–6 aliquots taken from the ion exchange chromatography (resource Q) as showed in (C). (B) Affinity chromatography using Ni–Sepharose high performance. (C) Ion exchange chromatography (resource Q).

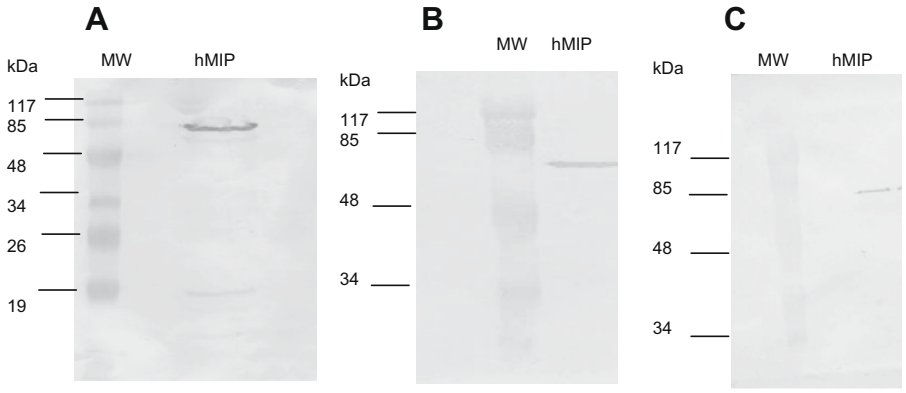

Fig. 2. Western blotting assays for *h*MIP. (A) Assay with the antibody against the poly-histidine tag. (B) Assay using the antibody against full-length *h*MIP. (C) Assay using the antibody against the *h*MIP N-terminal synthetic peptide.

in the Western blotting experiments *h*MIP was recognized by three different antibodies, i.e., the polyclonal anti-hexahistidine tag antibody (Fig. 2A), the polyclonal anti-MIP raised against GST-MIP (Fig. 2B), and the polyclonal anti-MIP raised against the *h*MIP N-terminal synthetic peptide (Fig. 2C).

Structural characterization

The tertiary and secondary structures of the obtained recombinant *h*MIP were analyzed using fluorescence and far-UV CD.

The blue shifted maximum intensity of the *h*MIP intrinsic fluorescence emission spectrum at 331 nm (Fig. 3A), indicated that most likely, the Trp residues of the analyzed protein are predominantly in hydrophobic environments. This could be further confirmed, denaturing the protein at 50 °C, when the Trp residues were exposed to the polar environment of the solvent (water) its intrinsic fluorescence decreased with the incubation time at this elevated temperature (Fig. 3B). What is characteristic of correctly folded globular proteins.

The CD spectrum of the recombinant *h*MIP is shown in Fig. 3C. *h*MIP form 3 different batches were analyzed and the spectra from both of these samples were very similar. The content of secondary structure was estimated by deconvoluting the spectra of *h*MIP: α-helix 11.1 ± 0.6%; antiparallel β-sheet 31.7 ± 1.4%; parallel β-sheet 5.7 ± 0.1%; β-turn 18.5 ± 0.2%; random coil 35.1 ± 0.1%. These results are consistent with those expected from correctly folded proteins. The spectrum of an unfolded protein presents an intense characteristic negative band at ~200 nm, not observed in the *h*MIP far-UV CD spectra as shown in Fig. 3C, what result in higher percentages of random structures [16] than that verified here for the recombinant *h*MIP. The correct folding of the protein is also supported by the fact that the specific activities from both batches were highly similar.

Characterization of the enzymatic activity

MIP removes eight N-terminal residues from imported mitochondrial protein precursors [3–5]. The ornithine transcarbamoylase intermediate (M-iOTC) has been used as a substrate for MIP activity assays [11]. However, for this work, we took advantage of a previous observation that MIP can also hydrolyze the nonapeptide, bradykinin (RPPGFSPFR) [17]. Although probably this peptide is not a natural substrate for MIP, measuring the hydrolysis of bradykinin-like synthetic peptides is clearly a simpler and easier method to evaluate the peptidase activity of *h*MIP. In addition, bradykinin and its respective synthetic peptide analogues have been used to characterize the two most studied peptidases from the MIP family (M3 of the metallopeptidases), i.e., the TOP and NEL [18–21]. Therefore, two of these bradykinin-derived FRET peptides, Abz-RPPGFSPFRQ-EDDnp and Abz-GFSPFRQ-EDDnp, were assayed with *h*MIP as substrates. The groups Abz–EDDnp represent the donor–acceptor fluorescence pair where Abz is *ortho*-aminobenzoic acid and EDDnp is *N*-(2,4-dinitrophenyl) ethylenediamine.

Recombinant *h*MIP hydrolyzed bradykinin at the ...F↓S... peptide bond, which is the same cleavage site that has been previously described [17]. The other peptidases from MIP family, i.e., TOP and NEL, also cleave bradykinin at the same site (RPPGF↓SPFR) [18,19]. Interestingly, recombinant *h*MIP hydrolyzed both bradykinin FRET derived substrates, Abz-RPPGFSPFRQ-EDDnp and Abz-GFSPFRQ-EDDnp at the ...F–S... bond, differently to TOP and NEL that cleave the FRET substrates at ...P–F... Table 1 shows the cleavage sites at bradykinin and the FRET derived peptides by MIP, TOP and NEL.

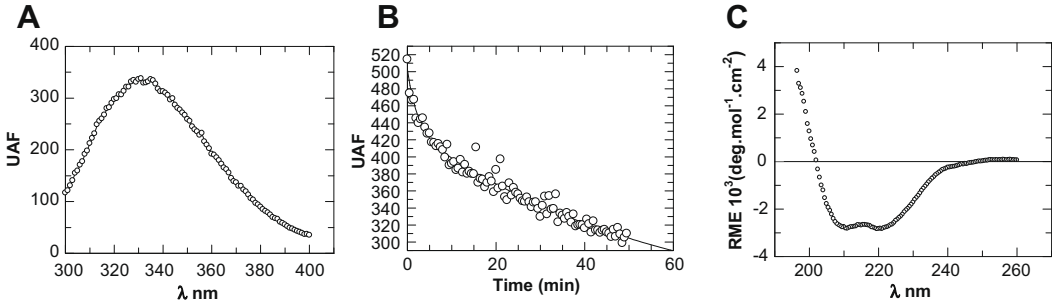

Fig. 3. (A) Fluorescence emission spectrum of *h*MIP (λ_{EX} = 280 nm), showing a maximum emission at λ_{EM} of 331 nm. (B) Time course of thermal denaturation for *h*MIP incubated at 50 °C, evaluated using fluorescence emission measurements (λ_{EX} = 280 nm; λ_{EM} = 331 nm). The curve is a non-linear regression plot using a double exponential decay equation (two phases). UAF, arbitrary unit of fluorescence. (C) The CD spectrum of *h*MIP. MRE, mean residue molar ellipticity.

Table 1
The cleavage sites at bradykinin, Abz-RPPGFSPFRQ-EDDnp and Abz-GFSPFRQ-EDDnp by TOP, NEL and *h*MIP. The cleaved sites are indicated by ↓.

	(Bradykinin) RPPGFSPFR	Abz-RPPGFSPFRQ-EDDnp	Abz-GFSPFRQ-EDDnp
*h*MIP	RPPGF↓SPFR	Abz-RPPGF↓SPFRQ-EDDnp	Abz-GF↓SPFRQ-EDDnp
TOP	RPPGF↓SPFR	Abz-RPPGFSP↓FRQ-EDDnp	Abz-GFSP↓FRQ-EDDnp
NEL	RPPGF↓SPFR	Abz-RPPGFSP↓FRQ-EDDnp	Abz-GFSP↓FRQ-EDDnp

Using the Abz-GFSPFRQ-EDDnp the enzymatic activity of recombinant *h*MIP was measured in the presence of DTT (Fig. 4) and various protease inhibitors (Table 2).

The effect of different DTT concentrations on *h*MIP activity is a distinguish feature of this peptidase as well as of TOP [22,23]. Fig. 4 shows the k_{cat}/K_M ratio of hydrolysis of Abz-GFSPFRQ-EDDnp by *h*MIP determined in the presence of increasing DTT concentrations. At low concentrations (<100 μM) DTT activates *h*MIP but at higher concentrations DTT inhibits the enzyme activity. The kinetic parameters for the hydrolysis of Abz-GFSPFRQ-EDDnp by *h*MIP were determined in the presence of the optimum DTT concentration observed (100 μM): K_M = 1.0 μM; k_{cat} = 0.04 s^{-1}; k_{cat}/K_M = 40 mM^{-1} s^{-1}. In addition to the different cleavage site *h*MIP hydrolyzed this substrate with an efficiency 12.5-fold lower than NEL and 65-fold lower than TOP [19]. But, despite this relatively low susceptibility of this FRET substrate by *h*MIP, future developments may lead to improved FRET substrates, for instance, based on predicted MIP cleavage regions of mitochondrial protein precursors.

The *h*MIP was inhibited totally by *ortho*-phenanthroline (10 mM), 90% inhibited by EDTA (10 mM), and inhibited significantly by bestatin (10 μM). A small effect was observed with PMSF, and no inhibition was detected with E-64 (Table 2). As expected, this inhibition profile is highly consistent with a metallopeptidase such as *h*MIP. JA-2 (a TOP inhibitor) [21], captopril (an angiotensin-converting enzyme inhibitor) [24] or thiorphan (a neprilysin inhibitor) [25] presented lower affinities by *h*MIP in comparison with the respective target enzymes of these inhibitors (Table 3). These results are of special interest because these compounds are potent metallopeptidase inhibitors that are used widely to measure TOP, ACE (angiotensin-converting enzyme) or NEP (neprilysin) enzymatic activity in cells and/or tissue samples, and also for *in vivo* treatments.

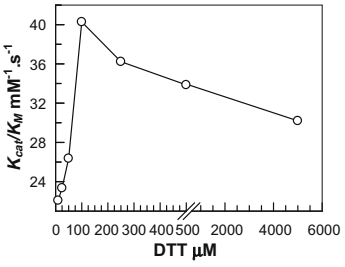

Fig. 4. Effect of DTT concentration on the catalytic efficiency of Abz-GFSPFRQ-EDDnp hydrolysis by *h*MIP.

Table 2
The effect of inhibitors on the hydrolytic activity of recombinant *h*MIP.

Inhibitor (concentration)	Relative hydrolysis rate (%)
Control with no inhibitor	100
E-64 (10 μM)	100
EDTA (10 mM)	10
Bestatin (10 μM)	58
PMSF (1 mM)	84
ortho-Phenanthroline (10 mM)	0

Table 3
Inhibition constants for *h*MIP by JA-2, captopril and thiorphan. The K_i values for the correspondent specific metalopeptidase target of each inhibitor were also shown for comparison.

Inhibitor	K_i (μM)	
	MIP	Inhibitor enzyme target
JA-2	7.7	[a]TOP – 0.045 [a]NEL – 0.534
Captopril	57	[b]ACE – 0.046
Thiorphan	1.5	[c]NEP – 0.01

K_i values [a]from Ref. [21], [b]from Ref. [24] and [c]from Ref. [25].

Conclusions

Taken together, the data presented here demonstrate the expression of recombinant *h*MIP in *E. coli*. The purified recombinant enzyme was active and properly folded.

The activity assay with the bradykinin-derived FRET substrates described herein is the first description of a continuous method for MIP activity measurement [18,19]. FRET substrates are useful tools to evaluate the substrate specificity of MIP, an important step for the development of specific inhibitors, given that it has been proposed that the inhibition of MIP could attenuate some complications of Friedreich ataxia a neurodegenerative disease [17].

MIP is a good target for structural studies because its 3D structure has not been determined to date. Therefore, the expression strategy employed here can contribute to further biochemical and structural studies of this protease.

Acknowledgments

This work was supported by FAPESP and CNPq. We thank Dr. Aparecida Tanaka (UNIFESP, SP, Brazil) for critical suggestions of this manuscript.

References

[1] M. van der Laan, M. Rissler, P. Rehling, Mitochondrial preprotein translocases as dynamic molecular machines, FEMS Yeast Res. 6 (2006) 849–861.
[2] O. Gakh, P. Cavadini, G. Isaya, Mitochondrial processing peptidases, Biochim. Biophys. Acta 1592 (2002) 63–77.
[3] Y. Gavel, G. von Heijne, Cleavage-site motifs in mitochondrial targeting peptides, Protein Eng. 4 (1990) 33–37.
[4] G. Isaya, F. Kalousek, W.A. Fenton, L.E. Rosenberg, Cleavage of precursors by the mitochondrial processing peptidase requires a compatible mature protein or an intermediate octapeptide, J. Cell Biol. 113 (1991) 65–76.
[5] F. Kalousek, J.P. Hendrick, L.E. Rosenberg, Two mitochondrial matrix proteases act sequentially in the processing of mammalian matrix enzymes, Proc. Natl. Acad. Sci. USA 85 (1988) 7536–7540.
[6] S.S. Branda, G. Isaya, Prediction and identification of new natural substrates of the yeast mitochondrial intermediate peptidase, J. Biol. Chem. 270 (1995) 27366–27373.
[7] G. Isaya, F. Kalousek, L.E. Rosenberg, Sequence analysis of rat mitochondrial intermediate peptidase: similarity to zinc metallopeptidases and to a putative yeast homologue, Proc. Natl. Acad. Sci. USA 89 (1992) 8317–8321.
[8] A. Chew, E.A. Buck, S. Peretz, G. Sirugo, P. Rinaldo, G. Isaya, Cloning, expression, and chromosomal assignment of the human mitochondrial intermediate peptidase gene (MIPEP), Genomics 40 (1997) 493–496.
[9] G. Isaya, D. Miklos, R.A. Rollins, MIP1, a new yeast gene homologous to the rat mitochondrial intermediate peptidase gene, is required for oxidative metabolism in *Saccharomyces cerevisiae*, Mol. Cell. Biol. 14 (1994) 5603–5616.
[10] G. Isaya, W.R. Sakati, R.A. Rollins, G.P. Shen, L.C. Hanson, R.C. Ullrich, C.P. Novotny, Mammalian mitochondrial intermediate peptidase: structure/function analysis of a new homologue from *Schizophyllum commune* and relationship to thimet oligopeptidases, Genomics 28 (1995) 450–461.
[11] A. Chew, R.A. Rollins, W.R. Sakati, G. Isaya, Mutations in a putative zinc-binding domain inactivate the mitochondrial intermediate peptidase, Biochem. Biophys. Res. Commun. 226 (1996) 822–829.

[12] A. Chew, G. Sirugo, J.P. Alsobrook 2nd, G. Isaya, Functional and genomic analysis of the human mitochondrial intermediate peptidase, a putative protein partner of frataxin, Genomics 65 (2000) 104–112.
[13] I.Y. Hirata, P. Boschcov, M.C. Oliveira, M.A. Juliano, A. Miranda, J.R. Chagas, S. Tsuboi, Y. Okada, L. Juliano, Synthesis of human angiotensinogen (1–17) containing one of the putative glycosylation binding sites and its hydrolysis by human renin and porcine pepsin, Int. J. Pept. Protein Res. 38 (1991) 298–307.
[14] C.K. Brown, K. Madauss, W. Lian, M.R. Beck, W.D. Tolbert, D.W. Rodgers, Structure of neurolysin reveals a deep channel that limits substrate access, Proc. Natl. Acad. Sci. USA 98 (2001) 3127–3132.
[15] K. Ray, C.S. Hines, J. Coll-Rodriguez, D.W. Rodgers, Crystal structure of human thimet oligopeptidase provides insight into substrate recognition, regulation, and localization, J. Biol. Chem. 279 (2004) 20480–20489.
[16] G. Bohm, R. Muhr, R. Jaenicke, Quantitative analysis of protein far UV circular dichroism spectra by neural networks, Protein Eng. 5 (1992) 191–195.
[17] N.D. Rawlings, F.R. Morton, C.Y. Kok, J. Kong, A.J. Barrett, MEROPS: the peptidase database, Nucleic Acids Res. 36 (2008) D320–325.
[18] V. Oliveira, M. Campos, J.P. Hemerly, E.S. Ferro, A.C. Camargo, M.A. Juliano, L. Juliano, Selective neurotensin-derived internally quenched fluorogenic substrates for neurolysin (EC 3.4.24.16): comparison with thimet oligopeptidase (EC 3.4.24.15) and neprilysin (EC 3.4.24.11), Anal. Biochem. 292 (2001) 257–265.
[19] V. Oliveira, M. Campos, R.L. Melo, E.S. Ferro, A.C. Camargo, M.A. Juliano, L. Juliano, Substrate specificity characterization of recombinant metallo oligopeptidases thimet oligopeptidase and neurolysin, Biochemistry 40 (2001) 4417–4425.
[20] E.J. Lim, S. Sampath, J. Coll-Rodriguez, J. Schmidt, K. Ray, D.W. Rodgers, Swapping the substrate specificities of the neuropeptidases neurolysin and thimet oligopeptidase, J. Biol. Chem. 282 (2007) 9722–9732.
[21] M.F. Machado, V. Rioli, F.M. Dalio, L.M. Castro, M.A. Juliano, I.L. Tersariol, E.S. Ferro, L. Juliano, V. Oliveira, The role of Tyr605 and Ala607 of thimet oligopeptidase and Tyr606 and Gly608 of neurolysin in substrate hydrolysis and inhibitor binding, Biochem. J. 404 (2007) 279–288.
[22] C.N. Shrimpton, M.J. Glucksman, R.A. Lew, J.W. Tullai, E.H. Margulies, J.L. Roberts, A.I. Smith, Thiol activation of endopeptidase EC 3.4.24.15. A novel mechanism for the regulation of catalytic activity, J. Biol. Chem. 272 (1997) 17395–17399.
[23] F. Kalousek, G. Isaya, L.E. Rosenberg, Rat liver mitochondrial intermediate peptidase (MIP): purification and initial characterization, EMBO J. 11 (1992) 2803–2809.
[24] M.C. Araujo, R.L. Melo, M.H. Cesari, M.A. Juliano, L. Juliano, A.K. Carmona, Peptidase specificity characterization of C- and N-terminal catalytic sites of angiotensin I-converting enzyme, Biochemistry 39 (2000) 8519–8525.
[25] R. Tran-Paterson, G. Boileau, V. Giguere, M. Letarte, Comparative levels of CALLA/neutral endopeptidase on normal granulocytes, leukemic cells, and transfected COS-1 cells, Blood 76 (1990) 775–782.